Estimation of Sparse Magnetic Susceptibility Distributions from MRI using Non-linear Regularization

B. Kressler[1,2], L. de Rochefort[2], P. Spincemaille[2], T. Liu[1,2], and Y. Wang[1,2]

[1]Department of Biomedical Engineering, Cornell University, Ithaca, New York, United States, [2]Department of Radiology, Weill-Cornell Medical College, New York, New York, United States

INTRODUCTION

Magnetic susceptibility has important effects in MRI, generating both contrast and artifacts. A technique to quantitatively estimate magnetic susceptibility distributions could potentially enable novel imaging applications, such as accurate quantification of cells labeled with superparamagnetic iron oxide particles. However, recovering the susceptibility distribution from standard MR images is an ill-conditioned deconvolution problem and is difficult to solve in general. In this work, we present an approach for generating susceptibility images from field maps in MRI using non-linear regularization techniques.

METHODS

In image space, the effect of a magnetic susceptibility distribution can be described through convolution of the distribution with a dipole response, which in k-space becomes point-wise multiplication with the kernel $(1/3 - k_z^2/K^2)$, where K is the k-space radius. Estimation of the susceptibilities of specific regions using the singular value decomposition of the image space convolution has been previously proposed [1], but the SVD technique is too computationally expensive for susceptibility estimation of every voxel in an image. Given the relative field map ψ in parts per million, the volume susceptibility distribution χ for every voxel in the image can in theory be estimated as $\chi = FT^{-1}[(1/3 - k_z^2/K^2)^{-1}FT(\psi)]$ [2]. However, straightforward inversion in this manner is ill-conditioned because of the zeros in the k-space kernel (points where $k_z^2/K^2 = 1/3$). One approach to ill-conditioned problems is Tikhonov regularization, where the least squares problem $\min_\chi\|C\chi-\psi\|^2$ is modified to $\min_\chi\|C\chi-\psi\|^2+\alpha^2\|R\chi\|^2$, where C is the matrix representation of the image space convolution, α is a tunable regularization parameter, and R is a regularization matrix. In standard Tikhonov regularization, R is the identity matrix, though other choices such as an approximation to the image space gradient are possible. Tikhonov regularization has been previously applied to inversion of susceptibility distributions and preliminary results, while encouraging, suffer from artifacts and underestimated regression slopes in quantifying susceptibilities [3].

Here we propose the use of non-linear regularization techniques, where the least squares problem is modified to $\min_\chi\|C\chi-\psi\|^2+\beta f(\chi)$ where $f(\chi)$ can be the ℓ_1 norm of χ or the three dimensional total variation of χ, given by $TV(\chi) = \Sigma_{(x,y,z)}\sqrt{[(\chi_{(x,y,z)}-\chi_{(x-1,y,z)})^2+(\chi_{(x,y,z)}-\chi_{(x,y-1,z)})^2+(\chi_{(x,y,z)}-\chi_{(x,y,z-1)})^2]}$. The ℓ_1 norm promotes sparsity in the estimated distribution while the total variation promotes sparsity of edges (i.e. favors regions of uniform susceptibility) in image space [4].

To validate the regularization techniques, two phantom studies were performed. In the first, 7 thin walled plastic tubes were attached vertically in a Petri dish. The dish and tubes were filled with water and imaged to provide a background reference phase map. The water in the tubes was replaced with Gd-DTPA (326 ppm/M at room temperature [5]) of varying concentrations (Fig. 1), and the dish was imaged again to provide the susceptibility distribution of interest. In the second experiment, a small plastic container was filled with 2% agar containing small pieces of agar gel with 100:1 Feridex. An identical container containing only 2% agar provided a reference phase map. Imaging was performed using a 1.5T GE Signa scanner and a 3D gradient echo sequence. For the 7 tube phantom, pulse sequence parameters were TR 50 ms, TE_1 1.6 ms, TE spacing 0.5 ms, 10 TEs, RBW 62.5 kHz, flip angle 30, matrix size 128x128x16, resolution 0.75x0.75x1mm. For the Feridex phantom, pulse sequence parameters were TR 50 ms, TE_1 2.6 ms, TE spacing 1 ms, 10 TEs, RBW 31.25 kHz, flip angle 30, matrix size 128x128x32, resolution 0.5x0.5x0.5 mm. Inversions were compared using ℓ_2, ℓ_2 of the gradient, ℓ_1, and total variation regularizations. Tikhonov regularized inversions used the conjugate gradients method, and inversions with non-linear regularization used a non-linear conjugate gradients algorithm [6].

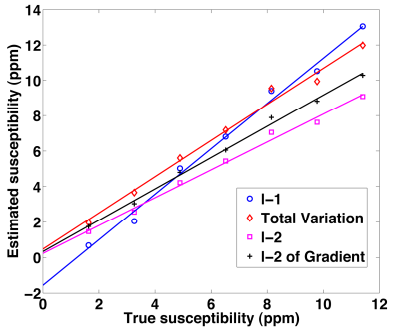

Figure 1. Plots of estimated susceptibility vs. true susceptibility for all regularization techniques.

RESULTS

Plots of the estimated susceptibilities vs. the true susceptibilities for the Gd phantom (Fig. 1) indicate a linear relationship between true susceptibility and the susceptibility measured by all four techniques. Parameters for the fit lines are listed in Table 1. Figure 2 shows images reconstructed using each inversion technique. The non-linear regularization techniques provide sharper depiction of the regions with high susceptibility.

Estimated susceptibility distributions for the agar gel containing Feridex are shown in Fig. 3. All inversion schemes provide good depiction of the susceptibility map, though the non-linear techniques provide slightly sharper delineation of boundaries and the ℓ_1 inversion has the least visible streaking artifacts.

	slope	y-intercept	r^2
ℓ_1	1.28	-1.56	0.993
Total Variation	1.02	0.47	0.988
ℓ_2	0.78	0.23	0.992
ℓ_2 of Gradient	0.88	0.34	0.996

Table 1. Parameters for the lines fit in Fig. 1.

DISCUSSION

In this work, we have compared four regularization techniques to invert arbitrary magnetic susceptibility distributions from magnetic field maps. The estimated susceptibilities have a linear relationship with respect to the true susceptibilities. However, the slopes slightly differ from unity. Some variation in slope is expected as a result of regularization type and parameter, although this could be calibrated and corrected for. Interestingly, a small overall offset was observed, which may result from the fact that a solution with any offset provides the same shifts, so that susceptibilities relative to the surrounding medium can be quantitatively assessed.

The susceptibility quantification techniques presented are targeted primarily towards estimation of sparse distributions or edges. These techniques may therefore allow accurate tracking of labeled cells, or homogeneous organs with well defined boundaries.

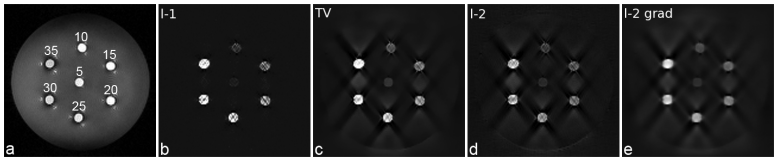

Figure 2. a) T_1 weighted image of the Gd phantom. Gd concentrations are listed in mM. Susceptibility distributions estimated using (b) ℓ_1, (c) total variation, (d) ℓ_2, and (e) ℓ_2 of the gradient regularization.

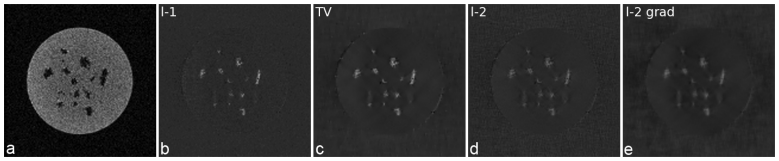

Figure 3. a) T_2 weighted image of the Feridex phantom. Susceptibility distributions estimated using (b) ℓ_1, (c) total variation, (d) ℓ_2, and (e) ℓ_2 of the gradient regularization.

CONCLUSION

The regularization techniques examined have different characteristic effects on the generated images. In these datasets, the ℓ_1 regularization produced susceptibility maps with the least streaking artifacts in the background. The ℓ_2 of the gradient regularization generated images with the least variance over the regions containing the susceptibilities of interest. Total variation regularization yielded the most accurate estimation of susceptibilities, having the regression slope closest to unity.

REFERENCES

[1] Li, et. al. MRM, 51:1077-1082, 2004. [2] Haacke, et. al. MRI, 23:1-25, 2005. [3] Morgan, et. al. ISMRM, 15:35, 2007. [4] Candes, et. al. Comm. Pure Appl. Math., LIX:1207-1223, 2006. [5] CRC Handbook of Chemistry and Physics, CRC Press, 2007. [6] Fletcher, et. al., Comput. J., 7:149-154, 1964.